Proceedings of the 33rd European Safety and Reliability Conference (ESREL 2023)
Edited by Mário P. Brito, Terje Aven, Piero Baraldi, Marko Čepin and Enrico Zio
©2023 ESREL2023 Organizers. *Published by* Research Publishing, Singapore.
doi: 10.3850/978-981-18-8071-1_P493-cd

Analysis of Road Transport Networks Travelled by both Internal Combustion and Electric Vehicles and Subject to Traffic Congestion due to Incident Scenarios

Lida Naseh Moghanlou
Energy Department, Politecnico di Milano, Via La Masa 34, 20156, Milano, Italy. E-mail: lida.naseh@polimi.it
Francesco Di Maio
Energy Department, Politecnico di Milano, Via La Masa 34, 20156, Milano, Italy. E-mail: francesco.dimaio@polimi.it
Enrico Zio
MINES Paris-PSL, Centre de Recherche sur les Risques et les Crises (CRC), France, enrico.zio@mines-paristech.fr
Department of Energy, Politecnico di Milano, Milan, Italy, enrico.zio@polimi.it

In this work, we use Finite State Machine (FSM) and Cell Transmission Model (CTM) for the analysis of a road transportation network travelled by both Internal Combustion Vehicles (ICVs) and Electric Vehicles (EVs). The application to a realistic network shows that FSM catches better than CTM the traffic volume changes when accidents occur, but paying the price of a larger computational cost. CTM, instead, averages the vehicles motion, thus somehow overlooking traffic congestions and travel time delays that would result in extra energy consumptions and EVs charging demand.

Keywords: Road Transportation Network, Accident Scenarios, Internal Combustion Vehicle (ICV), Electric Vehicle (EV), Single-Vehicle Model, Flow-Vehicle Model, Finite State Machine (FSM), Cell Transmission Model (CTM).

1. Introduction

Single-vehicle and flow-vehicle models have been proposed to describe vehicle motion in a road network (Anderson, and Nair, 2019), (Mu, et al., 2014).

Single-vehicle models are typically based on queuing theory to capture the driving patterns of individual vehicles in the system (Anderson, and Nair, 2019). Flow-vehicle models take a broader perspective than single-vehicle ones, treating vehicles as a collective flow (Mu, et al., 2014), (Wang, et. al., 2019). To name few examples of single-vehicle models, (Mu, et al., 2014) presented an Origin-Destination (O-D) model combined with Monte Carlo simulation for estimating the Electric Vehicle (EVs) charging load within a Spatial-Temporal Model (STM) framework; (Tang, et. al., 2016) analysed how EVs mobility impacts on the characteristics of a power network (in terms of Level of Congestion (LoC), Nodal Voltage Deviation (NVD) and Energy Loss Rate (ELR)); (Hou, et. al., 2016) proposed a rectangular coordinate road model for simulating EV motion that, in combination with a bidirectional charging control strategy, is used to assess the reliability of an integrated road-power infrastructure; (Anderson, and Nair, 2019) utilized FSM to model EV motion on transport networks to optimally schedule the charging of long-range batteries.

Flow-vehicle models describe vehicles motion based on an "integral" perspective (Mu, et al., 2014), (Wang, et. al., 2019), (Sun, et. al., 2018). They can be classified in Deterministic Fluid Dynamic Models (DFDMs), Static User Equilibrium Models (SUEMs) and Cell Transmission Models (CTMs). For example, (Bae, and Kwasinski, 2011) used a DFDM based on the conservation equation of traffic flow for assessing charging demand in charging stations; (Chen, et. al., 2020) used a SUEM for the optimal design of charging station location and capacities; (Wang, et. al., 2018) proposed a SUEM to simulate realistic traffic flows in transportation networks; (He, et. al., 2014) proposed a SUEM that considers also travellers recharging decisions, and captures the impact of recharging time and anxiety of drivers on travel time and route selection; (Xie and Jiang, 2016) developed a SUEM for modelling congested regional transportation networks where recharging or battery-swapping stations for EVs are scarce; (Wang, et. al., 2018) considered a CTM for modelling the interactions between a time-varying

urban transportation system and a power distribution system; (Wang, et. al., 2019) modelled a highway traffic flow by a CTM, to evaluate the spatial-temporal EV charging loads in different areas of an electrified transportation system.

In this study, we consider Finite State Machine (FSM) and Cell Transmission Model (CTM) as representative of single-vehicle and flow-vehicle models, respectively, for the analysis of a road transport network travelled by both of EVs and Internal Combustion Vehicles (ICVs), and subject to traffic congestion because of random incidents.

The rest of the paper is organized as follows. Section 2 briefly describes the FSM and CTM models. Section 3 presents the case study of a realistic road network; Section 4 presents the results of the study. Finally, Section 5 concludes the paper.

2. Vehicles Flow Modelling Approaches

In this Section, FSM and CTM are tailored for capturing the motion of vehicles on a road transport network, under both nominal conditions and disruption scenarios.

The road transport network is modelled as a connected graph $G(\mathcal{V}; \bar{\bar{\varepsilon}}; \bar{\bar{A}}; \bar{\bar{C}})$ (Anderson, and Nair, 2019), where $\mathcal{V} = \{1, 2, \dots, i, \dots, H\}$ is a non-empty set of H nodes, $\bar{\bar{\varepsilon}}$ is a matrix whose element ε^{ij} is the edge (road) length connecting the i-th and the j-th nodes (i=1, …, H and j=1, …, H, with $i \neq j$), $\bar{\bar{A}}$ is a weighted adjacency matrix, whose element a^{ij} is the number of lanes connecting the i-th and the j-th nodes, and $\bar{\bar{C}}$ is the capacity matrix, whose element c^{ij} is the maximum number of vehicles which can drive between the i-th and the j-th nodes at the same time. We consider that the road network is composed of a set of R road sections $\mathcal{R}$ = (1, 2, …, R, …, R), where a set of X charging stations CS = (CS_1 , CS_2, …, CS_x, …, CS_X) are present.

Power feeding the charging stations is modelled as a single-phase AC power flow that solves the dispatchment problem for an undirected graph $Q(W, Z)$ comprised of a set of buses W={$w_1, w_2 \dots, w_x, \dots, w_X$}, each one feeding a charging station CS_x and a set of branches Z (for both FSM and CTM). In FSM, power demand $CH_x(t)$ at the x-th charging station CS_x at time t, is calculated from Equation (1):

$$CH_x(t) = \sum_{r=k} ch_r\ (t) \qquad (1)$$

where $ch_r(t)$ is the power demand of the r-th EV being charged at time t, and k is the total number of EVs charged in CS_x. In CTM, the charging demands are approximated by the following linear function:

$$CH_x(t) = N_{\mathrm{R}}^{cl_i}(t).\alpha.r(t).P \qquad (2)$$

where $N_{\mathrm{R}}^{cl_i}(t)$ is the number of vehicles contained in cell cl_i of R-th road section, α is the EV penetration i.e., the portion of EVs on the road transport network, $r(t)$ is the probability of EV charging at time t and P is the charging power.
The power demand $E^{tot}(t)$ of the entire system at time t is calculated as:

$$E^{tot}(t) = \sum_{tot=1}^{X} CH_x(t) \qquad (3)$$

2.1. Finite State Machine

FSM models the process of state transition in time of a system (Monteiro, and Oliveira, 1998). For modelling EVs and ICVs motion on a road network, a FSM with six states S= {$S_0, S_1, S_2, S_3, S_4, S_5$} (Fig. 1) is here taken from (Naseh Moghanlou, et. al., 2021). Besides the initial "start-up" state S_0 and "shut-down" state S_3, we consider a "driving" state S_1 and a "queuing for traffic" state S_2, a "charging" or "refilling" state S_4 and a "queuing for charging" or "queuing for refilling" state S_5. In general terms, the generic r-th EV, EV_r, or p-th ICV, ICV_p, starts the trip with an entrance State of Charge (SoC), $SoC_r(t_{r,in})$, or Fuel Level (FL), $FL_p(t_{p,in})$, at its entrance time $t_{r,in}$ or $t_{p,in}$, and is found at time t in the edge i,j ($i \neq j$) with state S_m according to the transition rule $f(S_m, i, \bar{\theta})$, which depends on:

$$\bar{\theta} = \left\{N_{\mathrm{R}}^{i+1,j+1}(t),\ SoC_r(t)\ or\ FL_p(t),\ N_{CS_x}(t)\ or\ N_{GS_\xi}(t)\right\}$$

where $N_{\mathrm{R}}^{i+1,j+1}(t)$ is the number of vehicles occupying the edge $i+1, j+1$ of road R at time t, $SoC_r(t)$ or $FL_p(t)$ is the SoC or FL of $EV_r\ or\ ICV_p$ at time t, and $N_{CS_x}(t)\ or\ N_{GS_\xi}(t)$ is the number of the EVs or ICVs which are charging or refilling in the x-th charging station CS_x or ξ-th gas station GS_ξ at time t. In practical words, we model the motion dynamics so that when a generic EV_r or ICV_p of the pool of N_{EVs} EVs or N_{ICVs} ICVs starts a trip, it switches from state S_0 to state S_1 if the number of vehicles occupying the next edge at time t, $N_{\mathrm{R}}^{i+1,j+1}(t)$, is smaller than the edge maximum capacity of vehicles $c^{i+1,j+1}$; whereas, it switches from S_0 to S_2, if $N_{\mathrm{R}}^{i+1,j+1}(t)$ is equal to $c^{i+1,j+1}$, i.e., the edge has reached its maximum capacity and cannot accommodate other vehicles. As $EV_r\ or\ ICV_p$ moves forward on edge i,j where the charging station CS_x or gas station GS_ξ is

located, if $SoC_r(t)$ or $FL_p(t)$ is at the lowest critical value, $SoC_{critical}$ for EVs or $FL_{critical}$ for non-commercial ICVs or $FL_{critical-c}$ for commercial ICVs, it may switch to state S_4 in order to recharge or refill, unless the number of EVs charging in $CS_x, N_{CS_x}(t)$ or the number of ICVs refilling in $GS_\xi, N_{GS_\xi}(t)$ at time t is equal to the maximum capacity of vehicles for that charging station, $C_{CS_x}^{max}$ or gas station, $C_{GS_\xi}^{max}$: in this case, EV_r or ICV_p switches to state S_5 and only later switches to state S_4 to recharge or refill when $N_{CS_x}(\mathrm{t}) < C_{CS_x}^{max}$ or $N_{GS_\xi}(t) < C_{GS_\xi}^{max}$. Besides taking into account the diversity of EVs battery type B_r, we also consider the driver charging attitude, $ch_r(t)$, which describes the fact that each EV driver has a specific preference value of SoC at which to recharge. Upon charging or refilling completion, EV_r *or* ICV_p switches to state S_1 and continues the trip, switching among its states according to the transition rules $f(S_m, i, \bar{\theta})$ and finally reaching the destination node at which time it switches to state S_3. In synthesis, the states transition rules $f(S_m, i, \bar{\theta})$ for the *r*-th EV at time *t*, are formulated as:

$$f(S_m, i, \bar{\theta}) = \begin{cases} S_{m+1} = S_1 \;\; if \;\; N_{\mathrm{R}}^{i+1,j+1}(t) < c^{i+1,j+1} \\ S_{m+1} = S_2 \;\; if \;\; N_{\mathrm{R}}^{i+1,j+1}(t) = c^{i+1,j+1} \\ S_{m+1} = S_4 \;\; if \;\; SoC_r(\mathrm{t}) \le SoC_{critical} \;\; and \;\; N_{CS_x}(\mathrm{t}) < C_{CS_x}^{max} \\ S_{m+1} = S_5 \;\; if \;\; SoC_r(\mathrm{t}) \le SoC_{critical} \;\; and \;\; N_{CS_x}(\mathrm{t}) = C_{CS_x}^{max} \end{cases} \quad (4)$$

Also, for each EV_r, the SoC can be evaluated in time as described by Equation (5), making explicit the dependence of the S_m on the sequence from start-up state S_0 to shut-down state S_3:

$$SoC_r(t) = \begin{cases} SoC_r(\mathrm{t}-\mathrm{T}) - P_d.T & S = S_1 \\ SoC_r(\mathrm{t}-\mathrm{T}) - P_q.T & S = S_2 \\ SoC_r(\mathrm{t}-\mathrm{T}) + P.T & S = S_4 \\ SoC_r(\mathrm{t}-\mathrm{T}) & S = S_5 \end{cases} \quad (5)$$

where P_d and P_q are the power absorbed while driving and queuing for traffic, respectively, P is the charging power and T is the travel time interval.

The vehicles flow, at each time t is, thus, evaluated by collecting the number of EVs and ICVs, $N_{\mathrm{R}}^{i,j}(t)$, passing through (or stopping at) each node *i*, edge *i,j*, charging station CS_x and gas station GS_ξ, along with the following information:

- ID of the vehicle ICV_p, EV_r
- Entrance time of ICVs and EVs into the road transport network, $t_{p,in}$ and $t_{r,in}$, respectively
- EVs entrance SoC, $SoC_r(t_{r,in})$
- ICVs entrance FL, $FL_p(t_{p,in})$
- Drivers charging attitude, $ch_r(t)$
- SoC profile, $SoC_r(t)$
- Travel time for each vehicle, Tr_{EV_r}, Tr_{ICV_p}.

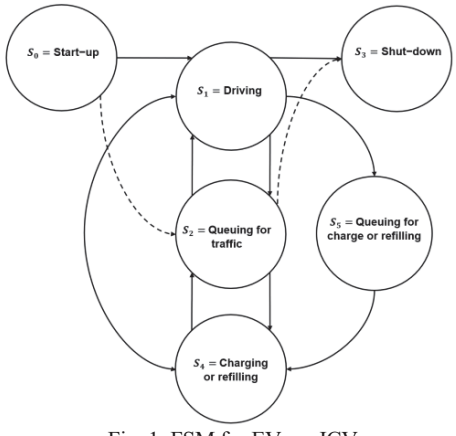

Fig. 1. FSM for EVs or ICVs

This allows collecting trajectories (i.e., time series) of travelled nodes and states (S_0, S_1, S_2, S_3, S_4, S_5) for each vehicle EV_r and ICV_p, traffic volume $N_{\mathrm{R}}^{i,j}(t), SoC_r(t), FL_p(t), N_{CS_x}(t)$ or $N_{GS_\xi}(t)$, $CH_x(t)$ for each edge *i,j*, charging station CS_x and gas station GS_ξ. The output of such multi-dimensional time series is the main value of the FSM with respect to flow-vehicle models that, instead, lump all this information in integral flow-related measures (Naseh Moghanlou, et. al., 2021).

2.2. Cell Transmission Model

The Cell Transmission Model (CTM) is widely used for modelling traffic flow in transportation systems (Wang, et. al., 2019). CTM considers the dynamics of traffic flow by modelling the movement of vehicles between adjacent cells $CL = \{cl_1, cl_2, \dots, cl_i, \dots, cl_H\}$, that are homogeneous sections of a network $\mathcal{H}$, where each cl_i represents a specific segment of the road, whose length cl^L is determined based on the average distance travelled by a typical vehicle in normal condition in one generic time interval T (similarly to the links $\varepsilon^{i,j}$ of the graph in FSM). The state of the system at each time *t* is defined as the number $N_{\mathrm{R}}^{cl_i}(t)$ of vehicles contained in the cell cl_i. The CTM reasoning is based on an intuitive balance equation, i.e., the number of vehicles in a cell at time t is equal to the sum of the number of

vehicles occupying it, plus the number of those incoming, minus those outgoing (Equation (6)):

$$n_i(t) = n_i(t-T) + \sum_{k \in \Pi^{-1}(i)} g_{k,i}(t) - \sum_{k \in \Pi^{+1}(i)} g_{i,j}(t) \quad (6)$$

where $\Pi^{-1}(i)$ and $\Pi^{+1}(i)$ denote the set of predecessor and successor cells of cell cl_i, $g_{k,i}(t)$ and $g_{i,j}(t)$ represent the number of vehicles flowing from cell *k* to cell *i* (i.e., incoming) and from cell *i* to cell *j* (i.e., outgoing) at time *t*, respectively. Depending on the type of cells (ordinary cell (CL_O), merging cell (CL_M), diverging cell (CL_D), source cell (CL_C) and sink cell (CL_S)), the updating rules are as follows (Daganzo, 1994), (Daganzo, 1995):

1) Ordinary Cell: for an *i*-th cell that has only one successor cell ($|\Pi^{+1}(i)|$=1) and one predecessor cell ($|\Pi^{-1}(i)|$=1), the incoming and outgoing flows at time *t* are, respectively:

$$g_{k,i}(t) = min\{\mathbb{F}_k(t), \mathbb{R}_k(t)\} \quad (7)$$

$$g_{i,j}(t) = min\{\mathbb{F}_i(t), \mathbb{R}_i(t)\} \quad (8)$$

where $\mathbb{F}$ and $\mathbb{R}$ are the maximum allowed outgoing and incoming flows:

$$\mathbb{F}_i(t) = min\{n_i(t), \mathfrak{f}_i(t)\} \quad (9)$$

$$\mathbb{R}_i = min\{n_i(t), (\omega/U[c^{cl_i}(t) - n_i(t)])\} \quad (10)$$

and $c^{cl_i}(t)$, $\mathfrak{f}_{cl_i}(t)$, ω and U are the maximum number of vehicles that can occupy cl_i, the maximum number of incoming and outgoing vehicles of cl_i, the backward wave speed, which is the speed with which disturbances propagate backward when traffic is congested, and the constant speed, respectively.

2) Merging Cell: for an *i*-th cell with two (or more) predecessor cells ($|\Pi^{-1}(i)| \geq 2$) and one successor cell ($|\Pi^{+1}(i)| = 1$), the outgoing flow $g_{i,j}(t)$ follows Equation (8), and the incoming flow $g_{k,i}(t)$ results from the solution of the maximization problem:

$$max \sum_{k \in \Pi^{-1}(i)} g_{k,i}(t) \quad (11)$$

subject to the constraints:

$$\begin{cases} g_{k,i}(t) \leq \mathbb{F}_k(t) \\ \sum_k g_{k,i}(t) \leq \mathbb{R}_i(t) \end{cases} \quad (12)$$

where the first equation states that the flow from the predecessor cell is constrained by its sending capacity, whereas the second equation states that the total incoming flows for all the predecessor cells should be lower than the receiving capacity of cell *i*.

3) Diverging Cell: for an *i*-th cell with one predecessor cell ($|\Pi^{-1}(i)| = 1$) and two (or more) successor cells (CL_D), the incoming flow $g_{k,i}(t)$ of the diverging cell follows Equation (7) and the outgoing flow $g_{i,j}(t)$ results from the solution of the maximization problem:

$$max \sum_{j \in \Pi^{+1}(i)} g_{i,j}(t) \quad (13)$$

subject to the constraints:

$$\begin{cases} g_{i,j}(t) \leq \mathbb{R}_i(t) \\ \sum_j g_{i,j}(t) \leq \mathbb{F}_j(t) \end{cases} \quad (14)$$

It is worth mentioning that the problem cannot be solved by a unique outgoing flow of a diverging cell, unless the turning parameter $\varphi_{i,j}(t)$ ($\forall j \epsilon \Pi^{+1}(i)$) is set to determine the rate at each time step. Equation (14) can be rewritten as follows:

$$\begin{cases} \varphi_{i,j}(t).\, g_{i,j}(t) \leq \mathbb{R}_j(t) \\ \sum_j g_{i,j}(t) \leq \mathbb{F}_j(t) \\ \sum_j \varphi_{i,j}(t) = 1 \end{cases} \quad (15)$$

4) Source and Sink Cells: the boundary conditions in the model are determined by the states of the sink (Cl_S) and source Cl_R cells, as well as the initial values of all cells. Sink cells have unlimited capacity i.e., $c^{Cl_S}(t) = \infty$ and can accept an unrestricted number of vehicles, with the incoming flow depending on the state of the predecessor cell. Source cells also have unlimited capacity i.e., $c^{Cl_R}(t) = \infty$ (typically following a user defined hourly pattern of vehicles flow), but their outgoing flow is finite, meaning that they can generate a specific amount of flow influenced by the successor cell characteristics ($\mathbb{F}_i(t)$ *and* $\mathbb{R}_i$).

2.1.3. Nominal Conditions Scenario

The nominal daily traffic conditions patterns are modelled as follow. In FMS, each vehicle, whether it is an EV or an ICV, begins its trip at the Origin (O) node with a certain state of charge (SoC) for EVs or fuel level (FL) for ICVs. During the journey, at each time interval *T*, the vehicle consumes power or fuel. When the vehicle passes by a charging station or gas station, it recharges or refills if the SoC or FL reaches a critical level that would prevent it from reaching the next charging station or gas station. Alternatively, when the vehicle reaches an intersection, it selects one of the available roads based on a driver turning rate

parameter φ. This travel cycle continues until the vehicle reaches the Destination (D).

In CTM, a fleet of the vehicles begins the trip at the Source cell and travels along the cells based on the CTM model. The approximation of the charging demands of EVs at a specific charging station is based on the number of EVs passing through, the EV penetration, the charging probability and the average rated charging power. Alternatively, when the vehicles reach an intersection, they select one of the available roads based on a turning parameter φ. This travel cycle continues until the vehicle reaches the sink cells.

2.1.4. Disruption Scenarios

Traffic congestion randomly occurs at a random edge or cell of the road network for a random duration ρ (hereafter also called severity), during which vehicles are temporarily trapped in a traffic jam. This is due to the occurrence of an incident whose key characteristics are the occurrence time, road capacity reduction, and duration. When an incident occurs, the road capacity is immediately reduced, potentially leading to traffic congestion if demand exceeds capacity. Once the incident is cleared, the road capacity recovers, and traffic conditions gradually return to normal.

In FSM, when a generic vehicle EV_r or ICV_p is stuck in the traffic jam (i.e., "queuing for traffic" state), it consumes P_q or F_p^{id} or F_{p-c}^{id} until it can move forward to the following road network node; when the vehicle reaches an intersection, the rule adopted for the "next road selection" is that the EV_r or ICV_p always takes the less crowded path, resulting in a shorter or longer path than the path travelled in the nominal conditions scenario. The charging or refilling logic is the same adopted for the nominal conditions travel.

3. Case Study

The case study used in (Wang, et. al., 2019) and (Naseh Moghanlou, et. al., 2021) is here adapted to the objective of the current study. The road transportation network is a comprehensive sample of a part of the national highway system of New York State, whose topological structure consists of R=11 road sections. The road network is mapped into the homogeneous graph G as shown in Fig. 2 (FSM) and the cells cl shown in Fig. 3 (CTM). In both cases, solid lines denote a direct connection between two nodes or cells, whereas dashed lines represent that some intermediate nodes or cells are omitted (for clarity sake). Vehicles can enter the road network either from node (or source cell) 1 or from node (or source cell) 22, and exit either from node (or sink cell) 203 or from node (or sink cell) 224. Along their routes, vehicles are modelled to drive at a constant speed of U = 65 mph.

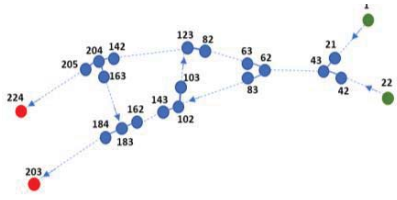

Fig. 2. Graph of the test road network (Naseh Moghanlou, et. al., 2021)

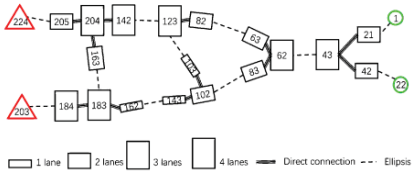

Fig. 3. Cells of test road network (Wang, et. al., 2019).

The nominal condition hourly traffic pattern adopted in is the one widely used as a benchmark traffic assignment model (Wang, et. al., 2019), (Naseh Moghanlou, et. al., 2021), and plotted in Fig. 4.

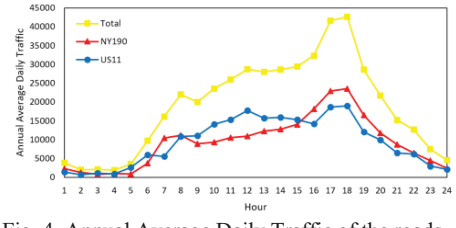

Fig. 4. Annual Average Daily Traffic of the roads

To compare FSM and CTM, and their sensitivity to the penetration of EVs in the road transportation network, different EV penetration levels (α = 25%, 50% and 75%) are considered. Table I summarizes the values of the parameters taken for the road transport network modelling.

In FSM, each EV is characterized by:

B_r: a random B_r following a truncated Normal distribution $\mathbb{N}(24,10)$, in the range of [10,90] (kWh) (*www.car-specs.net/ev-database.org*), (Su, et. al., 2011).

$SoC_r(t_{r,in})$: a random SoC uniformly distributed within the range of battery capacity B_r.

$ch_r(t)$: a random truncated Normal distribution $\mathbb{N}(20,10)$, in the range of [10 ,90] (kWh), corresponding to B_r distribution.

Charging time t_r^{ch}: a linear relationship between the charging time t_r^{ch} and the energy stored in the battery $ch_r(t)$, as described in Equation (16), (assuming that the drivers charging attitude $ch_r(t)$ and the charging power P of EVs are known (Wang, et. al., 2022)):

$$t_r^{ch} = \frac{ch_r(t)}{P} \qquad (16)$$

$SoC_{critical}$: 7 kWh, as the minimum SoC to reach the next charging station CS_{x+1}.

P_d: 17.38 kW, the driving power of EVs.

P_q: 6 kW, the queuing for traffic power of EVs.

In CTM, the average capacity of EVs battery is assumed to be 24 kWh. For simplicity, the charging probability is assumed to be constant and $r(t) = 0.7$.

It is assumed that a charging station (of unlimited maximum capacity) is located in the middle of each road section (X=11) providing the required power demand (Equation (3)), the charging power of EVs (P) is assumed equal to 75 kW.

TABLE I Parameters of the network

Parameters	Symbols	Values
Number of nodes	H	224
Edge length (*mi*)	$\varepsilon^{i,j}$	1.0833
Maximum number of vehicles per lane in the edge *i,j*	$c^{i,j}$	200
Number of cells	H	224
cell length (*mi*)	cl^L	1.0833
Maximum number of vehicles per lane in the cell *i*	c^{cl_i}	200
Maximum flow vehicle/min/lane)	$\mathfrak{f}_{cl_i}$	40
Turning parameter	φ	0.5
Travel time interval (*min*)	T	1

4. Results

4.1 Nominal Conditions Scenario

The results of the application of FSM and CTM, to the nominal conditions of traffic flow from 00:00 to 08:00 are first described. The number of vehicles per edges and cells are plotted in Figs. 5 and 6, respectively. FSM considers individual vehicles, rather than the overall flow of vehicles, and it is shown to have more accurate results than CTM and to be able to capture changes in traffic volume. However, the running time of FSM is more than five times that of CTM. For instance, the running time of FSM for the nominal scenario with percentage of EVs α=50% is 40 minutes whereas for the CTM, it is equal to 7 minutes on a CentOS (Intel(R) Xeon(R) CPU E5-2640 @2.40GHz and 17GB). This can become particularly relevant when the analysis is aimed at identifying critical roads where traffic congestion is more likely to occur which requires running several scenarios with varying parameters.

As an example of analysis, let us consider the changes in the power demand of the road network from 00:00 to 24:00 with different percentage of EVs (α=25%, 50%, and 75%). The results, in Fig. 7, illustrate the power demand when the CTM and FSM are used: since CTM provides an averaged motion of vehicles, it fails to capture the impact of traffic congestions, travel time delays and extra energy demand (that is indeed underestimated by CTM).

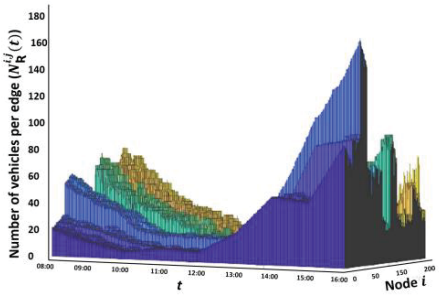

Fig. 5. Nominal condition of traffic flow with FSM: number of vehicles per edge of the transportation network from 8:00 to 16:00

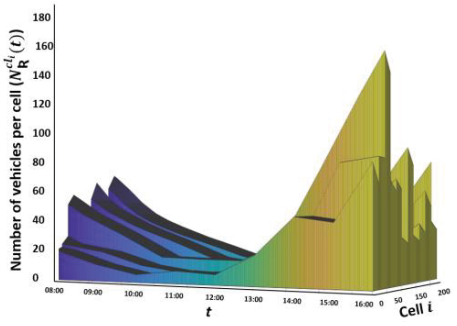

Fig. 6. Nominal condition of traffic flow with CTM: number of vehicles per cell of the transportation network from 8:00 to 16:00

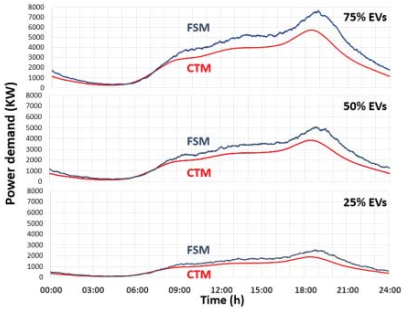

Fig. 7. Power demand when FSM and CTM are used to model nominal conditions under different EVs percentage α

4.1 Disruption Scenarios

Without loss of generality, we consider two disruption scenarios with severity ρ of 1 hour, and 2 hours, respectively. Both disruption scenarios are due to an incident occurring in edge 49,50 (cell 49) of road 3. In Fig. 8, the vehicles running per edge and per lane $\frac{N_R^{i,j}(t)}{a^{i,j}}$ obtained by FSM are plotted on a time span from 08:00 to 16:00 hours, for the cases of (a) normal conditions (b) ρ=1 hour disruption occurring at time 9:00 (i.e., rush time), (c) ρ=2 hours disruption occurring at time 9:00. In Fig. 9, the vehicles per cell and per lane $\frac{N_R^{cl_i}(t)}{a^i}$ estimated by CTM are plotted on a time span from 08:00 to 16:00 hours, for the cases of (a) normal conditions (b) ρ=1 hour disruption occurring at time 9:00 (i.e., rush time), (c) ρ=2 hours disruption occurring at time 9:00. Also in this case, FSM outperforms CTM in completely capturing changes in the traffic volume. However, FSM exhibits longer running times compared to CTM. For instance, the running time of FSM for ρ=1 with α=50% is 54 minutes whereas for CTM it is equal to 10 minutes, on a CentOS (Intel(R) Xeon(R) CPU E5-2640 @2.40GHz and 17GB).

Fig. 10 and Fig. 11 show additional insights provided by FSM that CTM does not give: the Probability Density Function (PDF) of vehicles travel time and delays, respectively, considering various levels of EVs percentage (α=25%, 50% and 75%). Again, it is shown that the FSM model captures the distribution of travel time, although with a higher computational effort. In contrast, CTM can only provide cumulative travel time information for the vehicles.

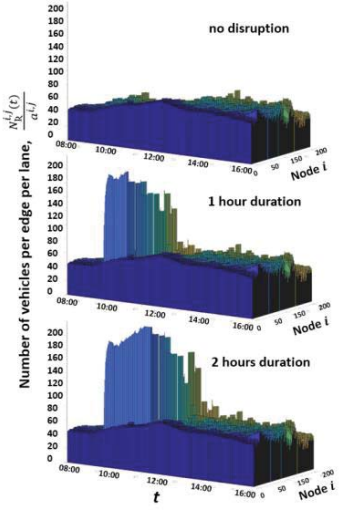

Fig. 8. Number of vehicles per lane estimated by FSM, in each edge of the transportation network from 8:00 to 16:00

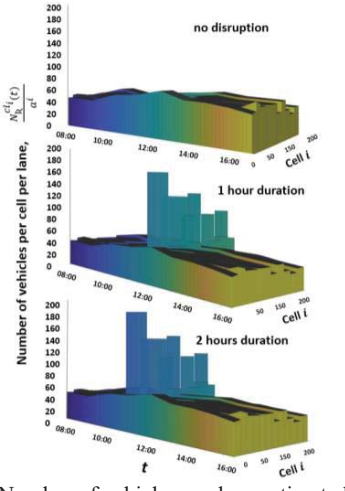

Fig. 9. Number of vehicles per lane estimated by CTM, in each cell of the transportation network from 8:00 to 16:00

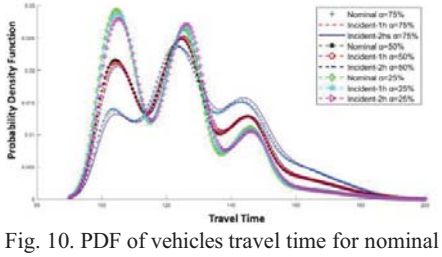

Fig. 10. PDF of vehicles travel time for nominal conditions and the considered disruption scenarios (using FSM)

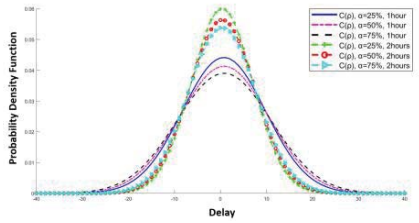

Fig. 11. PDF of vehicles delay due to the considered disruption scenarios (using FSM)

5. Conclusion

In this paper, we investigate the use of FSM and CTM for the analysis of road transport networks characterized by a mixture of EVs and ICVs. A realistic case study is considered under nominal conditions and disruption scenarios, for different levels of EVs percentage (α=25% 50% and 75%).

FSM allows modelling individual vehicles separately, thus, capturing their unique interactions and characteristics such as route choices, traffic congestion, and travel time delays. This allows providing a detailed analysis of individual vehicles motion and effectively capture changes in traffic flow, but at the expenses of long computation times. On the other hand, CTM provides an "integral" perspective on the vehicles motion by modelling the collective motion of vehicles within the road transportation system.

Acknowledgement

Lida Naseh Moghanlou acknowledges the financial support from the Energy for Motion Project "Dipartimenti Eccellenti 2018-2022", funded by MUR.

References

Gandoman, F.H., Ahmadi, A., Van den Bossche, P., Van Mierlo, J., Omar, N., Nezhad, A.E., Mavalizadeh, H. and Mayet, C., 2019. Status and future perspectives of reliability assessment for electric vehicles. Reliability Engineering & System Safety, 183, pp.1-16.

Naseh Moghanlou, L., Hoseyni, S.M., Di Maio, F. and Zio, E., 2021. Finite State Machine Modelling for The Performance Analysis of An Integrated Road-Power Infrastructure with A Hybrid Fleet of EVs And ICVs. In Proceedings of the 31st European Safety and Reliability Conference, ESREL 2021 (pp. 2716-2723).

Wang, H., Fang, Y.P. and Zio, E., 2019. Risk assessment of an electrical power system considering the influence of traffic congestion on a hypothetical scenario of electrified transportation system in new york state. IEEE Transactions on Intelligent Transportation Systems, 22(1), pp.142-155.

Mu, Y., Wu, J., Jenkins, N., Jia, H. and Wang, C., 2014. A spatial–temporal model for grid impact analysis of plug-in electric vehicles. Applied Energy, 114, pp.456-465.

Tang, D. and Wang, P., 2016. Nodal impact assessment and alleviation of moving electric vehicle loads: From traffic flow to power flow. IEEE Transactions on Power Systems, 31(6), pp.4231-4242.

Hou, K., Xu, X., Jia, H., Yu, X., Jiang, T., Zhang, K. and Shu, B., 2016. A reliability assessment approach for integrated transportation and electrical power systems incorporating electric vehicles. IEEE Transactions on Smart Grid, 9(1), pp.88-100.

Anderson, S. and Nair, V.J., 2019. Electric vehicle charge scheduling on highway networks from an aggregate cost perspective. arXiv preprint arXiv:1901.03017.

Wang, J., Peeta, S. and He, X., 2019. Multiclass traffic assignment model for mixed traffic flow of human-driven vehicles and connected and autonomous vehicles. Transportation Research Part B: Methodological, 126, pp.139-168.

Sun, C., Pei, X., Hao, J., Wang, Y., Zhang, Z. and Wong, S.C., 2018. Role of road network features in the evaluation of incident impacts on urban traffic mobility. Transportation research part B: methodological, 117, pp.101-116.

Bae, S. and Kwasinski, A., 2011. Spatial and temporal model of electric vehicle charging demand. IEEE Transactions on Smart Grid, 3(1), pp.394-403.

Chen, R., Qian, X., Miao, L. and Ukkusuri, S.V., 2020. Optimal charging facility location and capacity for electric vehicles considering route choice and charging time equilibrium. Computers & Operations Research, 113, p.104776.

Wang, X., Shahidehpour, M., Jiang, C. and Li, Z., 2018. Coordinated planning strategy for electric vehicle charging stations and coupled traffic-electric networks. IEEE Transactions on Power Systems, 34(1), pp.268-279.

He, F., Yin, Y. and Lawphongpanich, S., 2014. Network equilibrium models with battery electric vehicles. Transportation Research Part B: Methodological, 67, pp.306-319.

Xie, C. and Jiang, N., 2016. Relay requirement and traffic assignment of electric vehicles. Computer-Aided Civil and Infrastructure Engineering, 31(8), pp.580-598.

Wang, X., Shahidehpour, M., Jiang, C. and Li, Z., 2018. Resilience enhancement strategies for power distribution network coupled with urban transportation system. IEEE Transactions on Smart Grid, 10(4), pp.4068-4079.

Monteiro, J.C. and Oliveira, A.L., 1998, May. Finite state machine decomposition for low power. In Proceedings of the 35th annual Design Automation Conference (pp. 758-763).

Daganzo, C.F., 1994. The cell transmission model: A dynamic representation of highway traffic consistent with the hydrodynamic theory. Transportation research part B: methodological, 28(4), pp.269-287.

Daganzo, C.F., 1995. The cell transmission model, part II: network traffic. Transportation Research Part B: Methodological, 29(2), pp.79-93.

[Online]. Available: https://www.car-specs.net/ev-database.org [Accessed: March 2020].

Su, W., Eichi, H., Zeng, W. and Chow, M.Y., 2011. A survey on the electrification of transportation in a smart grid environment. IEEE Transactions on Industrial Informatics, 8(1), pp.1-10.

Wang, H., Abdin, A.F., Fang, Y.P. and Zio, E., 2022. Resilience assessment of electrified road networks subject to charging station failures. Computer-Aided Civil and Infrastructure Engineering, 37(3), pp.300-316.